

# A non-ideal second order thermal model with effects of losses for simulating Beta-type Stirling refrigerating machine

Muluken Z. GETIE<sup>a,b,c</sup>, Francois LANZETTA<sup>a</sup>, Sylvie BEGOT<sup>a</sup>, Bimrew T. ADMASSU<sup>c</sup>

<sup>a</sup>FEMTO-ST Institute, Univ. Bourgogne Franche-Comte, CNRS Parc technologique, 2 avenue Jean Moulin, F-90000 Belfort, France

<sup>b</sup>Bahir Dar Energy Center, Bahir Dar Institute of Technology, Bahir Dar University, Bahir Dar, Ethiopia

<sup>c</sup>Faculty of Mechanical and Industrial Engineering, Bahir Dar Institute of Technology, Bahir Dar University, Bahir Dar, Ethiopia

---

## Abstract

A key issue in the optimal designing of a Stirling machine is to develop a precise thermodynamic numerical model that could predict the performances and provide means for further optimization. In this paper, a non-ideal second-order numerical model called modified simple analysis model has been presented for the Stirling cycle refrigerating machine. The model incorporates effects of shuttle heat loss to the expansion space and mass leakage to the crankcase in the differential equations of pressure change, rate of change of mass of gas in compression and expansion spaces, and mass flow rates across these working spaces. The model was simulated using MATLAB code for Beta configuration FEMTO 60 Stirling engine operating as a refrigerator and validated with an experiment. The validation of the numerical model with experimental work showed that the results of the simulation are consistent with the results of the experiment. Hence, the numerical model could be used to design a Stirling cycle refrigerating machine for moderate temperature applications with reasonable accuracy especially if optimization is performed further. The effects of incorporating shuttle heat loss in the differential equations on the temperature of working gas and the overall performance of the Stirling refrigerator have been analyzed. Lastly, parametric investigations have also been performed to evaluate the effect of operating parameters (temperature, pressure, and frequency) on the performances of the refrigerating machine. Better performance could be achieved at relatively lower frequency or higher pressure.

*Keywords:* Stirling cycle refrigerator, thermal modeling, Beta configuration, Modified simple, Moderate cooling, Experiment

---

## Nomenclature

### General

$\dot{m}$  mass flow rate [kg.s<sup>-1</sup>]

$A$  cross sectional area [m<sup>2</sup>]

$A_{wg}$  wetted area of the metal [m<sup>2</sup>]

$C$  average molecular speed [m.s<sup>-1</sup>]

$C_p$  isobaric specific heat [J.kg<sup>-1</sup>.K<sup>-1</sup>]

$C_v$  isochoric specific heat [J.kg<sup>-1</sup>.K<sup>-1</sup>]

$D$  piston diameter [m]

$d$  hydraulic diameter [m]

$D_d$  diameter of displacer [m]

$f$  frequency [Hz]

$f_r$  Reynolds friction factor

$G$  mass flux [kg.m<sup>-2</sup>.s<sup>-1</sup>]

$h$  convective heat transfer coefficient [W.m<sup>-2</sup>.K<sup>-1</sup>]

$J$  annular gap between cylinder and piston/displacer [m]

$K$  heat conductivity [W.m<sup>-1</sup>.K<sup>-1</sup>]

$L$  length [m]

$m$  mass of working fluid [kg]

$m_{leak}$  mass leakage [kg]

---

\*Corresponding Author: Tel +33 753810328/ fax +33 38457820032

Email address: muluken.zegeye@bdu.edu.et (Muluken Z. GETIE)

$n$	rotational speed [rpm]
$N_{st}$	Stanton number
$NTU$	number of transfer unit
$NU$	Nusselt number
$P$	pressure [Pa]
$P_r$	Prandtl number
$P_{buffer}$	buffer space pressure [Pa]
$Q$	heat [J]
$Q_{rl}$	regenerator ineffectiveness heat loss [J]
$Q_{shut}$	shuttle heat loss [J]
$Q_{wrl}$	internal heat conduction loss [J]
$R$	gas constant [ $J.kg^{-1}.K^{-1}$ ]
$Re$	Reynolds number
$s$	stroke [m]
$T$	temperature [K]
$U_p$	linear velocity [ $m.s^{-1}$ ]
$V$	volume [ $m^3$ ]
$V_{swc}$	compression swept volume [ $m^3$ ]
$W$	work [J]
$W_{i,ad}$	ideal adiabatic work [J]

### Greek symbols

$\alpha$	phase angle [rad]
$\Delta$	difference
$\epsilon$	regenerator ineffectiveness
$\eta$	clearance efficiency
$\gamma$	ratio of specific heats, ( $C_p/C_v$ )
$\mu$	viscosity [Pa.s]
$\tau$	compression ratio
$\theta$	crank angle [rad]

### Subscripts

$c$	compression space
$cr$	chiller
$e$	expansion space
$g$	gas
$h$	hot heat exchanger
$r$	regenerator
$t$	total

## 1. Introduction

The Stirling machine is a type of the closed thermodynamic cycle machine invented in 1816 by Robert Stirling as a heat engine. The Stirling cycle refrigerator, which is the counterpart of the Stirling engine, was first recognized in 1832 [1]. The system was practically realized in 1862 when Alexander Kirk built and patented a closed cycle Stirling refrigerator [2]. Until 1949, it was reported that very little development occurred and when the Philips Company in Holland ran a Stirling engine in the reverse direction it liquefied air over the cold tip [3].

A detailed review of the Stirling refrigerating machines has been conducted for low and moderate temperature cooling applications [4]. In the research, the operating principle, configuration and driving mechanisms of Stirling refrigerator have been discussed in addition to research findings. Stirling cycle cooling devices with different configurations have been investigated by many researchers. All configurations are working with the same thermodynamic cycle but with different mechanical designs. Different configurations of the Stirling machine have a different compression ratio, making it more or less suitable for a specific application depending on the attainable temperature difference [5]. The research as pointed out that appropriate configuration and drive mechanism of the Stirling machine is one of the design criteria for the optimal performance.

The maximum cooling capacity was obtained when the volume ratio was almost equal to the temperature ratio for the developed beta type prototype refrigerator [6]. V-type Stirling-cycle refrigerator have been reported to have comparable COP with vapor compression refrigerating machine at near ambient cooling conditions [7]. The optimal relation between the cooling rate and the coefficient of performance of the Stirling cycle refrigerator was analyzed [8, 9, 10].

Tekin Y. et al [11] investigated the effect of regenerator porosity, phase angle, pressure, and speed on the performance of the refrigerating machine using different working fluids. The parameters, such as the power demand and the coefficient of performance were examined under different rotating speeds and charging pressures for a domestic cooling machine [12, 13]. Lean et al [13] reported that the COP varied between 0.1 and 0.9 under different working parameters and pressures. An isothermal model was developed for an Alpha type Stirling cycle cryocooler by considering various losses and the effects of different parameters on cooling performance were investigated [14]. From the research, it has been reported that the highest heat loss was due to conduction loss and the highest work loss was due to the mechanical friction loss. Theoretical and experimental evaluation of the Gamma-type Stirling refrigerator was conducted [15, 16].

The effects of parameters such as dead volume ratio, compression ratio, types of working fluids, and the phase angle on the performance of the Beta-type refrigerating

machine were studied [6]. An optimal refrigerating performance reported in a phase angle between  $96.1^\circ$  -  $108.32^\circ$  and the maximum cooling capacity is obtained when the volume ratio is almost equal to the temperature ratio. Hachem et al. [17] developed a thermodynamic model and conducted an experimental validation to optimize an air-filled Beta-type Stirling refrigerator. The researchers pointed out that the optimal values of regenerator diameter and length for the prototype Beta-type Stirling refrigerator are about 22 mm and 60 mm respectively.

Even though the Stirling cycle coolers with different configurations have been invented long years ago, the number of researches is still limited especially for domestic applications. The purpose of this paper was to develop a realistic numerical model for designing an air-filled domestic Stirling cycle refrigerator. Therefore, a new numerical model for the Beta-type Stirling cycle refrigerating machine called the modified simple model is presented, which has been developed by adapting and modifying engine models [18, 19] for refrigerating purpose. The differential equations have been modified by incorporating mass leakage and shuttle heat loss. The effects of these losses on the mass flow rate across the compression and expansion spaces have been considered for the first time. Furthermore, the effect of shuttle heat loss on the temperature of working gas and overall cooling performance has been also analyzed first by considering as a separate loss and then incorporating it in the differential equation. The other losses are separately treated in a modified adiabatic model. Since we could not compress air to the required pressure level in our laboratory, experimental validation was conducted using nitrogen for experiment and simulation using FEMTO 60 machine. Furthermore, the effects of operating parameters have been analyzed.

## 2. Mathematical modeling

### 2.1. Ideal adiabatic modeling

An ideal Stirling refrigeration cycle operates with four separate thermodynamic processes as seen Fig. 1, which consists of two isothermal processes (1-2 and 3-4) and two constant volume processes (2-3 and 4-1). The overall Stirling cycle refrigeration machine is configured into five control volumes (two working spaces and three heat exchangers) serially connected in the same way as described by [18]. The control volumes for the analysis include compression space(c), hot heat exchanger(h), regenerator(r), chiller(cr) and expansion space(e) as shown in Fig. 2. Hence, the ideal adiabatic model for Stirling refrigerator is simply adapted from [18] with all relevant assumptions. The set of governing ordinary differential equations for the Stirling cycle refrigeration machines are summarized in Table 1.

### 2.2. Modified ideal adiabatic analysis

The system of ideal adiabatic differential equations was modified by including the effects of gas leakage from work-

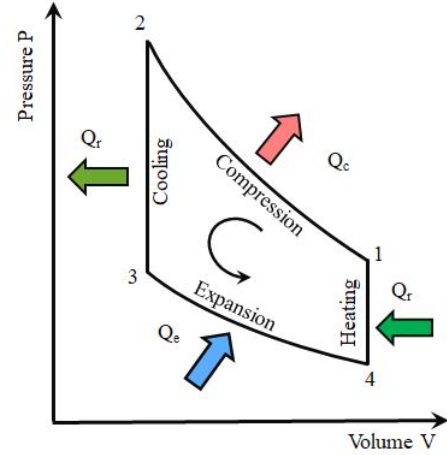


Fig. 1. Schematic PV diagram of an ideal Stirling refrigerator.

ing space to buffer space (crankcase) and shuttle heat loss by displacer from compression to expansion spaces for the Stirling cycle refrigerator by adapting and modifying the Simple-II engine model developed by [19]. The main reason for the inclusion of mass leakage and shuttle heat loss to the differential equation is because these losses could affect the overall working condition of working fluid. So, the differential equations of mass and energy conservation of the original ideal adiabatic model of the Stirling cycle refrigerator presented above have been modified by including the mass leakage loss and shuttle heat loss respectively. Other losses are not included directly in the modified ideal adiabatic simulation.

To accurately predict a Stirling cycle refrigeration machine performance and to design optimal machine for a specific application, a detailed investigation of various losses has to be considered as discussed in section 2.3. Different types of heat and power losses are shown in Fig. 3.

#### 2.2.1. Mass leakage loss

The design of seals in Stirling machines is somewhat complicated by the fact that the running of the machine in the working space should be dry, that is without oil. Furthermore, the bearing pressure of the seals should be limited to avoid local heating and friction losses. Stirling machine seal design therefore involves some compromise, which may result to gas leakage to some degree. Hence, studying the thermodynamic effect of mass leakage is one aspect of this design. The leakage loss is more critical especially at higher speed and higher pressure Stirling machines [20]. The original mass balance equation of ideal adiabatic model is modified by incorporating mass leakage loss from the working space to the buffer space as:

$$m_c + m_h + m_r + m_{cr} + m_e - m_{leak} = m_t \quad (1)$$

The amount of working gas lost per time from working

Table 1: Summary of ideal adiabatic model.

Parameters	equations
Pressure	$P = \frac{mR}{\frac{V_c}{T_c} + \frac{V_h}{T_h} + \frac{V_r}{T_r} + \frac{V_{cr}}{T_{cr}} + \frac{V_e}{T_e}}$ $dP = \frac{-P\gamma(\frac{dV_c}{T_{ch}} + \frac{dV_e}{T_{cre}})}{\frac{V_c}{T_{ch}} + \gamma(\frac{V_h}{T_h} + \frac{V_r}{T_r} + \frac{V_{cr}}{T_{cr}}) + \frac{V_e}{T_{cre}}}$
Mass	$m_i = \frac{PV_i}{RT_i} \text{ (where } i = c, h, r, cr, e)$
Change of mass	$dm_i = \frac{dp m_i}{p} = \frac{dp}{R} \frac{V_i}{T_i} \text{ (where } i = h, r, cr)$ $dm_c = \frac{pdV_c + \frac{V_c dp}{\gamma}}{RT_{ch}}$ $dm_e = \frac{pdV_e + \frac{V_e dp}{\gamma}}{RT_{cre}}$
Mass flow	$\dot{m}_{ch} = -dm_c, \quad \dot{m}_{hr} = \dot{m}_{ch} - dm_h$ $\dot{m}_{rcr} = \dot{m}_{cre} + dm_{cr}, \quad \dot{m}_{cre} = dm_e$
Conditional temperature	<p>If <math>m_{ch} &gt; 0, T_{ch} = T_c</math> if not <math>T_{ch} = T_h</math></p> <p>If <math>m_{cre} &gt; 0, T_{cre} = T_{cr}</math> if not <math>T_{cre} = T_e</math></p>
Temperature variation	$dT_e = T_e \left( \frac{dP}{P} + \frac{dV_e}{V_e} - \frac{dm_e}{m_e} \right)$ $dT_c = T_c \left( \frac{dP}{P} + \frac{dV_c}{V_c} - \frac{dm_c}{m_c} \right)$ $dQ_{h,i} = \frac{V_h dPC_v}{R} - C_p(T_{ch} \dot{m}_{ch} - T_h \dot{m}_{hr})$ $dQ_{r,i} = \frac{V_r dPC_v}{R} - C_p(T_h \dot{m}_{hr} - T_{cr} \dot{m}_{rcr})$
Energy	$dQ_{cr,i} = \frac{V_{cr} dPC_v}{R} - C_p(T_{cr} \dot{m}_{rcr} - T_{cre} \dot{m}_{cre})$ $W_{i,ad} = W_c + W_e$ $dW_{i,ad} = dW_c + dW_e \text{ where}$ $dW_c = PdV_c \text{ and } dW_e = PdV_e$

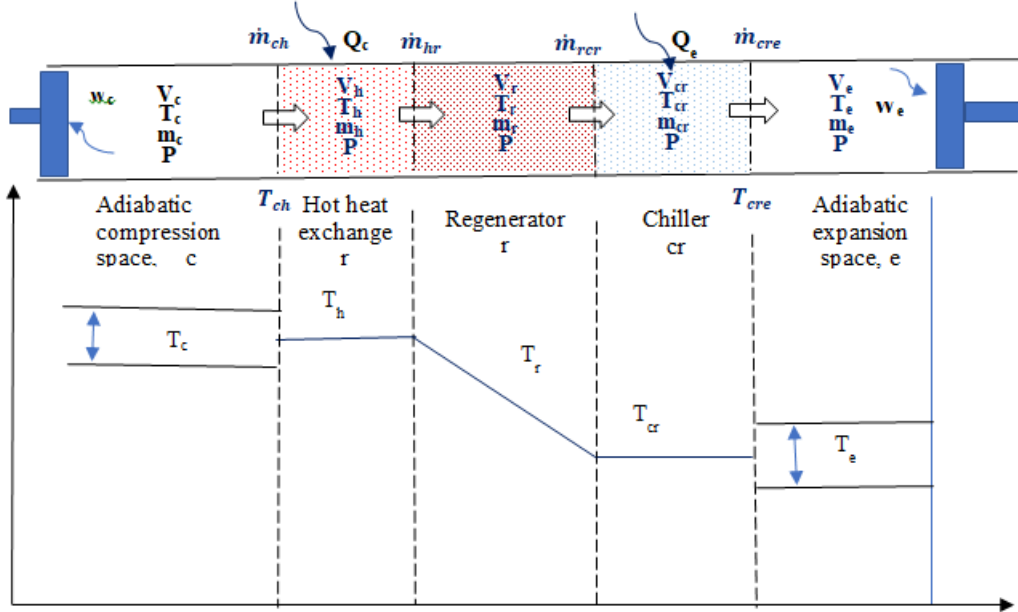


Fig. 2. Ideal adiabatic schematic model for Stirling cycle refrigerator with five cells and four interfaces.

space to the crank case is determined as [18]:

$$\dot{m}_{leak} = D\pi \frac{P + P_{buffer}}{4RT_g} \left( U_p J - \frac{J^3}{6\mu} \left( \frac{P - P_{buffer}}{L_p} \right) \right) \quad (2)$$

Differentiating Eq. 1, gives:

$$dm_c + dm_h + dm_r + dm_{cr} + dm_e - dm_{leak} = 0 \quad (3)$$

### 2.2.2. Shuttle heat loss

During its reciprocating movement, the displacer is frequently contacting with two temperature layers (compression and expansion space) of the working fluid. This effect leads the displacer motion to shuttle heat from hot end to cold end. The displacer absorbs heat at the hot end (compression side) of its stroke and gives off this heat at the cold end (expansion side). This loss mainly depends upon the nature of motion and the difference in temperature between the two sides.

The ideal adiabatic energy conservation equation is modified by including the shuttle heat loss as:

$$dQ_i - dQ_{shut} - dW_i = C_p(T_{i,o}\dot{m}_{i,o} - T_{i,in}\dot{m}_{i,in}) + C_v d(m_i T_i) \quad (4)$$

The shuttle heat loss ( $dQ_{shut}$ ) as given in [22, 23] is calculated as:

$$dQ_{shut} = \frac{\pi s^2 K_g D_d}{8JL_d} (T_c - T_e)$$

The change in mass in the compression and expansion spaces could be found by including the shuttle heat and leakage effects as:

$$dm_c = \frac{PdV_c + \frac{V_c dP}{\gamma}}{RT_{ch}} + \frac{dQ_{shut}}{C_p T_{ch}} + \dot{m}_{leak} \quad (5)$$

$$dm_e = \frac{PdV_e + \frac{V_e dP}{\gamma}}{RT_{cre}} - \frac{dQ_{shut}}{C_p T_{cre}} \quad (6)$$

Rearranging and substituting, the change in pressure is given as:

$$dP = \frac{-P\gamma \left( \frac{dV_c}{T_{ch}} + \frac{dV_e}{T_{cre}} \right) + \gamma R \frac{dQ_{shut}}{C_p} \left( \frac{T_{ch} - T_{cre}}{T_{ch} T_{cre}} \right) - 2\gamma R d\dot{m}_{leak}}{\frac{V_c}{T_{ch}} + \gamma \left( \frac{V_h}{T_h} + \frac{V_r}{T_r} + \frac{V_{cr}}{T_{cr}} \right) + \frac{V_e}{T_{cre}}} \quad (7)$$

Furthermore, particularly for the Beta-type configuration machine, shuttle heat and mass leakage could also affect the mass flow rate across the working spaces. Hence the mass flow rate across the compression and expansion spaces are respectively given as:

$$\dot{m}_{ch} = -dm_c - \frac{dQ_{shut}}{C_p T_{ch}} - \dot{m}_{leak} \quad (8)$$

$$\dot{m}_{cre} = dm_e - \frac{dQ_{shut}}{C_p T_{cre}} \quad (9)$$

The other equations remain the same as those of the ideal adiabatic model.

The actual performance of a refrigerator is determined following Fig. 4. The heat and power losses other than shuttle heat loss are presented in section 2.3. Power losses increase the power requirement. Therefore, the actual input power requirement ( $\dot{W}_a$ ) is evaluated as the sum of the ideal power and all power losses and given by:

$$\dot{W}_a = f(dW_{i,ad} + W_{fr} + W_{mec.fr} + W_{fin-sp}) + \dot{W}_{hys} \quad (10)$$

Heat losses cause the chiller to reject less heat. Then, the actual cooling power produced ( $Q_{cr,a}$ ) is computed as the difference between idealized cooling power and heat power losses from the system as:

$$\dot{Q}_{cr,a} = f(dQ_{cr,i} - Q_{wrl} - Q_{rl}) - \dot{Q}_{cond} - \dot{Q}_p - dQ_{shut} \quad (11)$$

Therefore, the actual COP could be found as:

$$COP = \frac{\dot{Q}_{cr,a}}{\dot{W}_a} \quad (12)$$

### 2.3. Modified simple analysis

The system of analysis of losses for the Stirling cycle refrigerator is adapted from the engine model [18]. The losses are classified into two categories based on their effect on this modified simple analysis. The first category of losses including regenerator ineffectiveness and fluid friction in the heat exchangers are differentially calculated with section 2.2 and applied to correct the working temperature. Then, losses such as power loss due to mechanical friction, conduction heat loss in the regenerator wall, pressure drop due to finite speed of piston, gas spring hysteresis loss, and pumping loss are evaluated as independent losses as they do not affect the operating condition.

#### 2.3.1. Heat loss due to internal conduction in the regenerator

The two heat exchangers work at different temperatures. Even though the temperature difference for domestic Stirling cycle refrigerators is not as large as in Stirling engines or cryocoolers, the internal conduction heat loss is not negligible. The amount of energy loss caused by internal heat conduction in the regenerator is found as follows [24, 25]:

$$Q_{wrl} = k \frac{A_{wg}}{L_f} (T_{wh} - T_{wcr}) \quad (13)$$

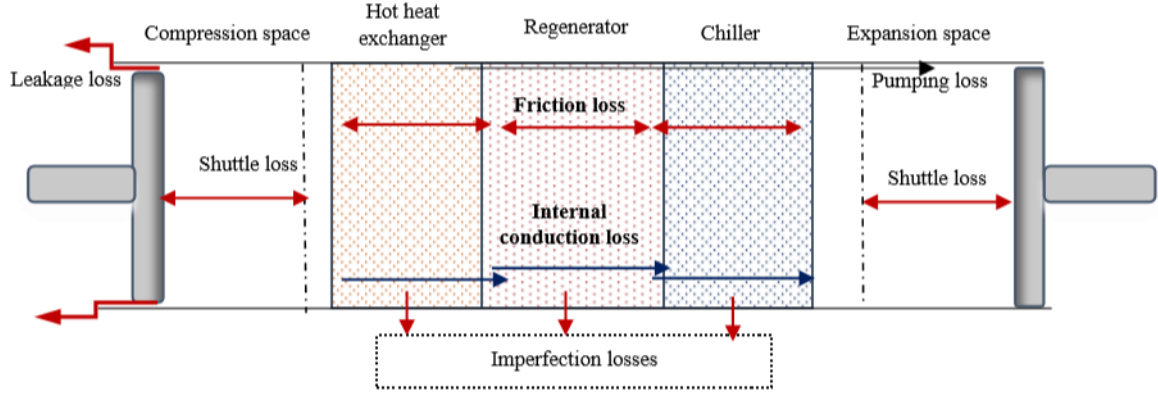


Fig. 3. Mapping of various heat and work losses (adapted from [21]).

### 2.3.2. Loss due to regenerator ineffectiveness/external conduction loss

For a non-ideal regenerator, when the working gas flows from the chiller to the hot heat exchanger, the gas will have the temperature somewhat lower than the hot heat exchanger. Due to the imperfection of the regenerator, the thermal energy loss is given by:

$$Q_{rl} = mc_p(1 - \epsilon)(T_c - T_e) \quad (14)$$

Where, based on [18], the ineffectiveness of the regenerator is defined as:

$$\epsilon = \frac{NTU}{NTU + 1} \quad (15)$$

$$NTU = N_{st} \frac{A_{wg}}{A} \quad (16)$$

and

$$N_{st} = 0.023Pr^{-0.6}Re^{-0.2} \quad (17)$$

Thus, the net heat absorbed from the chiller and net heat released to the hot heat exchanger per cycle are given by:

$$Q_{cr} = Q_{cr,i} - Q_{rl} = \frac{h_{cr}A_{cr}(T_{wcr} - T_{cr})}{f} \quad (18)$$

$$Q_h = Q_{h,i} + Q_{rl} = \frac{h_hA_h(T_{wh} - T_h)}{f} \quad (19)$$

Therefore, the heat exchanger temperatures are corrected using the wall temperature and the actual heat transfer as:

$$T_{cr} = T_{wcr} - \frac{fQ_{cr}}{h_{cr}A_{cr}} \quad (20)$$

$$T_h = T_{wh} - \frac{fQ_h}{h_hA_h} \quad (21)$$

Where,  $h = \frac{Nuk}{d}$ , is the convective heat transfer coefficient for both chiller and hot heat exchanger.

$Nu = 0.023Pr^n Re^{0.8}$  ( $n=0.3$  for hot heat exchanger and  $0.4$  for chiller) based on [18].

### 2.3.3. Losses due to pressure drop in heat exchangers

In the Stirling cycle machine, the friction losses in the heat exchangers result in pressure drops and lead to a reduction of performance. The pressure losses in heat exchangers are calculated to evaluate the amount of power losses due to drops in pressure. The amount of energy dissipated  $W_{fr}$  in regenerative Stirling cycle refrigerating machine due to pressure drops at the heat exchangers is evaluated as:

$$W_{fr} = \int_0^{2\pi} (\Delta P \frac{dV_c}{d\theta}) d\theta \quad (22)$$

Where,  $\Delta P = \Delta P_h + \Delta P_r + \Delta P_{cr}$  and

$\Delta P_i = \frac{2f_r \mu V_i G_i l_i}{m_i d_i^2}$  (Where  $i = h, r, cr$ )  $f_r$  is a product of Fanning friction factor and Reynolds number,  $Re$ .

$f_r$  for the regenerator (woven screen) has been evaluated from the correlations given by Gedeon and Wood [26] as:

$$f_r = 129 + 2.91Re^{0.897} \quad (23)$$

Then,  $f_r$  for chiller and hot heat exchangers is defined based on [18, 27] as:

$$f_r = 0.0791Re^{0.75} \quad (24)$$

### 2.3.4. Mechanical friction losses

Because of the relative motion between parts of the refrigeration machine, losses due to mechanical friction increases the amount of power input required for the process. The relative motions in such refrigerating machines include the joints in the displacer and the crank, between the piston and the crank, and between the crank and the axle of the prime mover. In addition, there is mechanical friction between the piston/displacer and the cylinder wall due to the fact that the piston/displacer does not move perfectly in its axial direction. Therefore, the power losses due to mechanical friction in one cycle is calculated by:

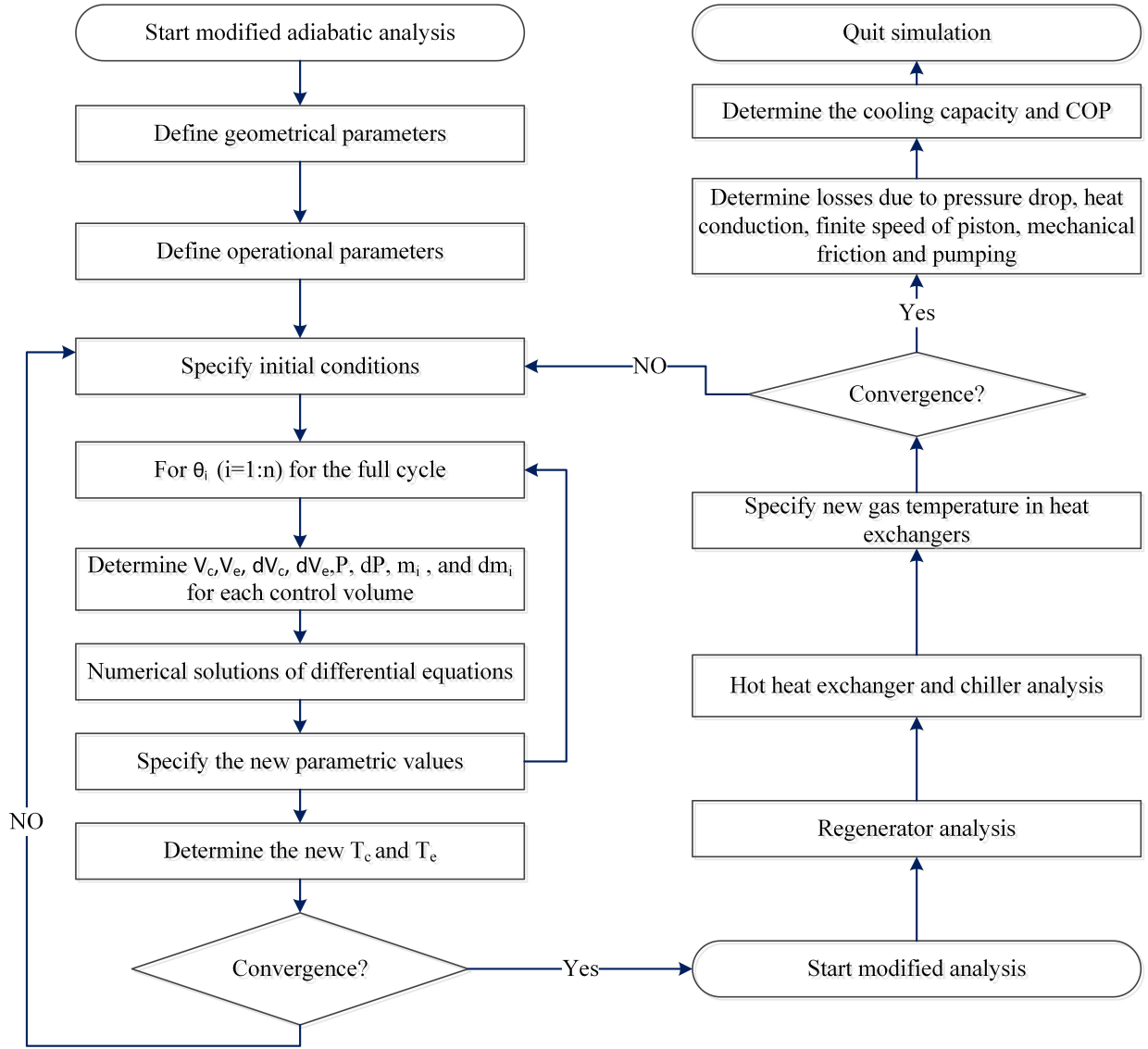


Fig. 4. Program flow chart of the model.

$$W_{mec.fr} = 2\Delta P_{mec.fr} V_{swc} \quad (25)$$

Where, pressure loss by mechanical friction is given in [28] as:

$$\Delta P_{mec.fr} = \frac{(0.4 + 0.0045sn)10^5}{3(1 - 1/3\tau)}(1 - 1/\tau) \quad (26)$$

### 2.3.5. Heat conduction losses

Due to temperature difference between compression and expansion spaces in Stirling cycle machines, which are separated by displacer, heat conduction occurred. The heat conduction losses are an additional loads for heat exchangers. The losses due to the heat of conduction during the refrigerating cycle is written as:

$$\dot{Q}_{cond} = k \frac{A}{L} \Delta T \quad (27)$$

### 2.3.6. Losses due to finite speed of piston

For the Stirling machine, the working spaces are periodically compressed and expanded by the piston and displacer. Based on the finite speed thermodynamic principle, the instantaneous pressure of compression and expansion spaces differs from the pressure in the respective piston surfaces. The work losses due to finite speed of piston in one cycle is evaluated by the product of pressure drop and the piston swept volume [14, 28].

$$W_{fin-sp} = 2\Delta p_{fin.sp} V_{swc} \quad (28)$$

and,

$$\Delta p_{fin.sp} = \frac{1}{2} \left( P \frac{a u_{p,c}}{C_c} + P \frac{a u_{p,e}}{C_e} \right)$$

$$a = \sqrt{3\gamma} \text{ and } C = \sqrt{3RT}$$

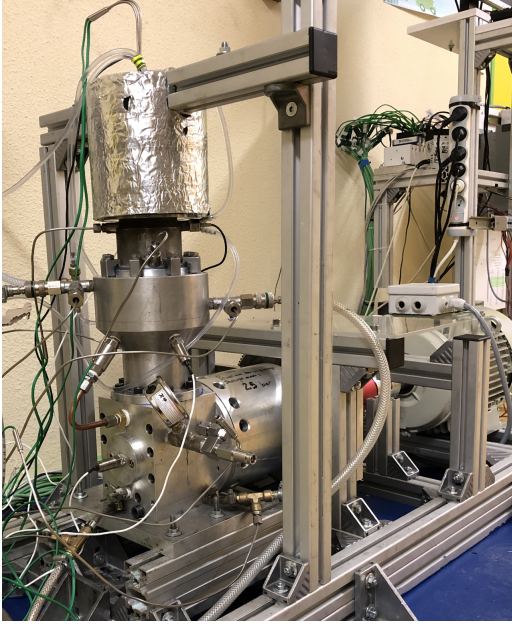


**Fig. 5.** Photo of refrigerating Stirling machine (Beta type) at cooling stage (FEMTO-ST laboratory)

### 2.3.7. Gas spring hysteresis losses

As the internal gas of the Stirling machine is compressed and expanded by the displacer, this internal gas could likely begin to act as a spring. This thermodynamic process is not recoverable and may introduce additional losses that could be in the form of the dissipation of the internal energy of the working fluid. This type of dissipation loss due to non-ideal character is modelled using the following expression [18]:

$$\dot{W}_{hys} = \sqrt{\frac{1}{32} \omega \gamma^3 (\gamma - 1) T_w P_{mean} k_g \left(\frac{V_d}{2V_t}\right)^2 A_{wg}} \quad (29)$$

### 2.3.8. Pumping losses

Because of the periodic variation of pressure throughout the working space of a Stirling cycle machine, the gap between the displacer and the cylinder wall can absorb and transfer gas from or to the expansion volume. The pumping losses are due to the fixed clearance volume existing between the displacer and the cylinder wall so that the displacer can move without rubbing. This leads to cooling loss in the refrigerating machine, named as pumping loss. Based on [14, 29] the pumping loss is given as;

$$\dot{Q}_p = (1 - \eta) \dot{m} C_p (T_c - T_e) \quad (30)$$

where:

$$\dot{m} = \frac{2f D_d L_d J}{R(T_c + T_e)} P_a$$

and

$$\eta = 1 - \frac{4\dot{m}^{0.6} C_p^{0.6} J}{3\pi k_g^{0.6} L_d^{0.6} D_d}$$

But, for a moderate temperature refrigeration machine, the temperature difference is very small compared to Stirling cryocoolers and heat engines, the pumping loss will be very small.

### 2.4. Solving method

The method of solving the numerical differential equations in section 2.2 initiated with taking the geometrical parameters and initial operating conditions as input parameters. The solution algorithm of the present numerical model has been illustrated by the flow chart in Fig. 4. The step of analysis was quite similar to the original ideal adiabatic model developed by Urieli [18], except the differential equations have been adapted to reverse cycle and corrected to include losses (shuttle heat and mass leakage). Variables and ordinary differential equations are solved for a full cycle. Schmidt analysis was used for the initial estimation of the mass of working gas and modified ideal adiabatic analysis to determine the working pressure and temperature. The classical fourth-order Runge Kutta method has been applied to solve the system of these differential equations.

In the model, void volumes of the three heat exchangers ( $V_h$ ,  $V_r$ , and  $V_{cr}$ ) were determined based on the geometrical specifications. The active volume variables including  $V_c$ ,  $V_e$ ,  $dV_c$ , and  $dV_e$  were obtained based on the configuration of the refrigerating machine as analytic functions of the crank angle  $\theta$ . Among the 24 variables, 11 variables and derivatives including  $Q_{shut}$ ,  $m_{leak}$ ,  $V_c$ ,  $V_e$ ,  $P$ ,  $m_c$ ,  $m_h$ ,  $m_r$ ,  $m_{cr}$ ,  $m_e$ , and  $W$  were analytically determined and the 7 derivatives were numerically integrated using the fourth-order Runge-Kutta method. The other 6 mass flow rate equations and boundary conditions are initial value problems. Initial gas temperatures in compression and expansion spaces were estimated as the hot heat exchanger and chiller temperatures, respectively. The numerical solution of differential equations was executed repeatedly until the steady-state condition is obtained.

As shown in Fig. 4, after completing the analysis of the modified ideal adiabatic model, the algorithm entered the second part of the analysis called modified simple analysis. In the modified simple analysis, the effect of regenerator ineffectiveness was considered to correct the hot heat exchanger and the chiller temperatures. The feedback was given to the numerical solution section by correcting the heat exchangers' temperature until the temperatures converge. Finally, the amount of the cooling production and the magnitudes of the required power input were corrected including the effect of all respective losses considered.

## 3. Experimental setup and validation

The numerical model presented above, was evaluated by considering the FEMTO 60 Stirling engine operating as a refrigerating machine as a case study. The photo of the cooling machine at cooling stage is shown in Fig. 5.

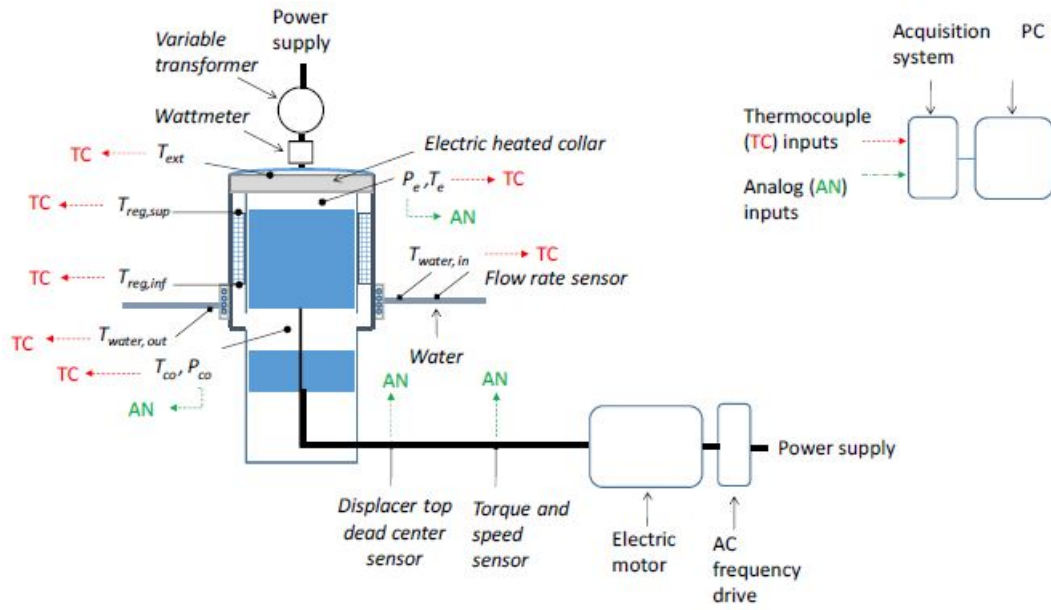


Fig. 6. Experimental setup for the measurement of the Stirling prototype.

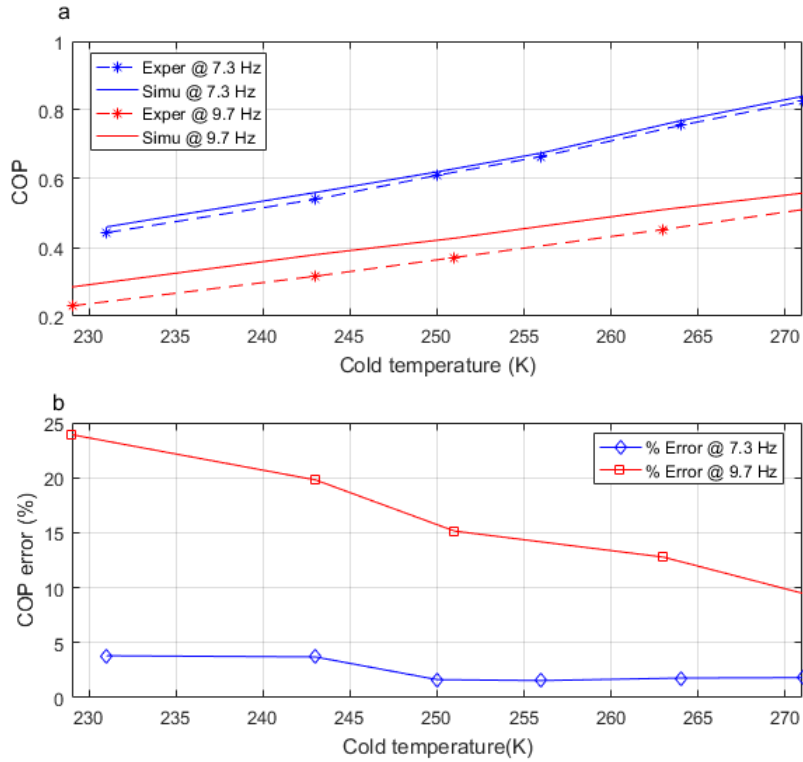
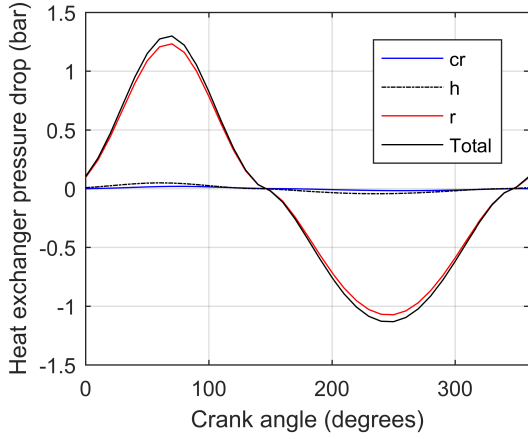
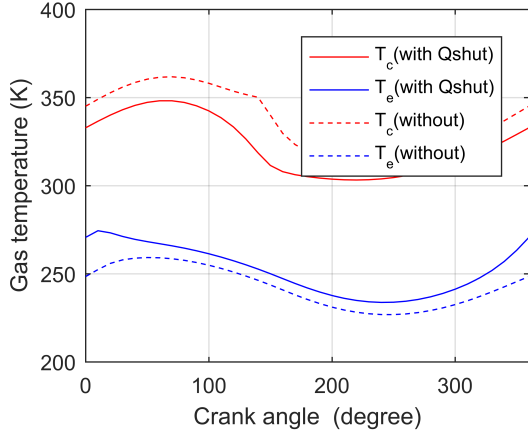


Fig. 7. Evaluating COP prediction accuracy of thermal model with experimental data.



**Fig. 8.** Heat exchanger pressure drop versus crank angle ( $P = 17.5$  bar,  $f = 7.5$  Hz).



**Fig. 9.** Gas temperature distribution in compression and expansion spaces (without means without including and with Qshut means with including shuttle heat loss in the differential equation).

The setup, the arrangement, and testing procedures of the experimental device were the same as described by [30] and are shown in Fig. 6. The working gas considered in the experiment was nitrogen, which is assumed to behave like a perfect gas. The main parameters and dimensions of the experimental device are tabulated in Table 2.

There are no more recognized experimental results for moderate temperature Stirling cycle refrigerator. Hence, this thermal model was validated with an experiment conducted at 7.3 Hz and 9.7 Hz for a series of cooling temperatures and a charging pressure of 17.5 bar using FEMTO 60 engine model. Fig. 7a and b depicted the comparison of COP and the associated relative error of non-ideal second-order thermal model (modified simple) with experimental values. Fig. 7a, demonstrates the comparison of the COP of the thermal model with experimental values for operating frequencies of 7.3 Hz and 9.7 Hz. From the figure, we could see that the COP for simulation result shows more

Table 2: Specifications of Stirling cooling machine used in this study.

No	Parameters	value
1	Hot heat temperature (K)	305
2	Cooling temperature (K)	270
3	Piston diameter (mm)	60
4	Displacer diameter (mm)	59
5	Piston stroke (mm)	40
6	Regenerator length (mm)	50
7	Diameter of regenerator (mm)	82
8	Compression space swept volume ( $\text{cm}^3$ )	103
9	Expansion space swept volume ( $\text{cm}^3$ )	113
10	Compression dead volume ( $\text{cm}^3$ )	4.24
11	Expansion dead volume ( $\text{cm}^3$ )	4.24
12	Working gas	Nitrogen
13	Frequency (Hz)	7.5
14	Charging pressure (bar)	20

closer values to experimental results at all temperature ranges in the case of 7.3 Hz than at 9.7 Hz. Fig. 7b, illustrates the relative error evaluated in predicting the COP of the prototype Stirling machine for an operating frequency of 7.3 Hz and 9.7 Hz. It has seen that the maximum relative prediction error of 23.9 % was found for an operating frequency of 9.7 Hz (as shown in Fig. 7b).

Generally, from Fig. 7 a and b, it could be confirmed that the present modified simple model predicts the cooling power and COP of the Stirling refrigerating machine for moderate cooling application with reasonable accuracy.

#### 4. Numerical results and discussion

In this paper, the Stirling cycle refrigerator with Beta configuration (FEMTO 60 Stirling engine working in reversed mode) and using air as a working fluid was investigated. The effect of incorporating shuttle heat loss in the differential equation was analyzed. Then comprehensive parametric study such as the effect of charging pressure, operating frequency, and temperature of cold space on the performance (input power requirement, cooling power produced, and COP) of the refrigerator were studied.

Fig. 8 shows the pressure drop across the hot heat exchanger, the regenerator, the chiller and the total pressure drop in all these heat exchangers versus the crank angle. As could be seen from the figure the pressure drop variation in the regenerator was much higher than the pressure drop in the other two heat exchangers. The maximum pressure drops for the regenerator and the total pressure drops were found respectively as 1.23 bar and 1.30 bar (at a charging pressure of 17.5 bar, frequency of 7.5 Hz, hot

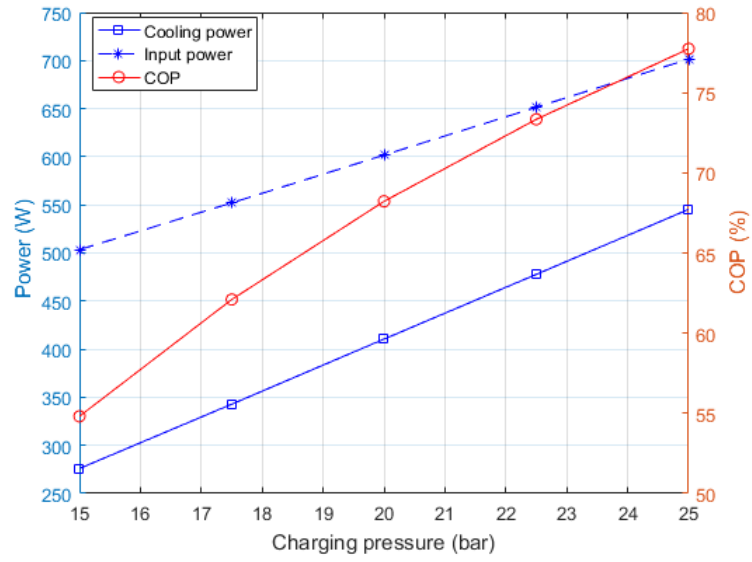


Fig. 10. Plot of Cooling performance Versus charging pressure ( $T_{cr} = 270$  K,  $T_h = 300$  K, and  $f = 7.5$  Hz).

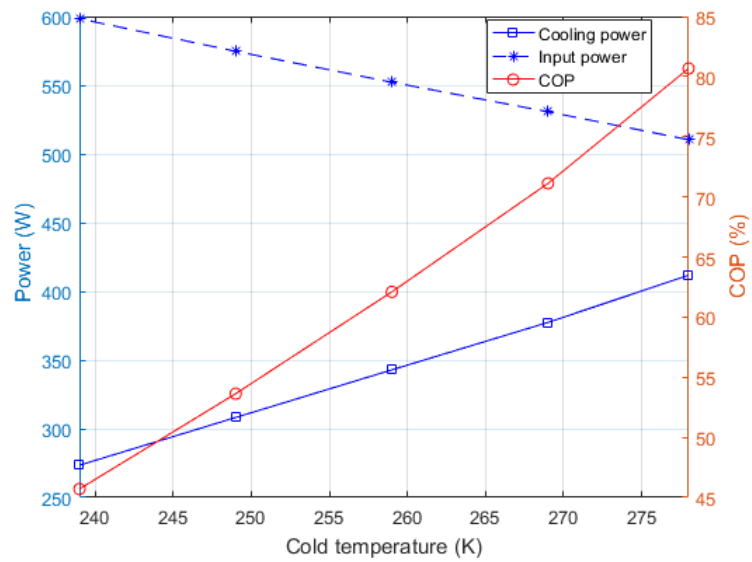
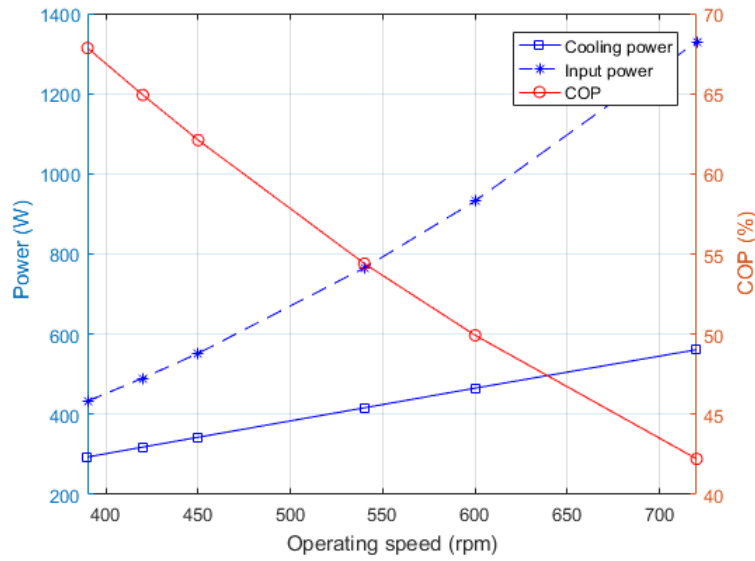


Fig. 11. Plot of Cooling performance Versus temperature of cold space ( $P = 17.5$  bar and  $f = 7.5$  Hz).



**Fig. 12.** Plot of Cooling performance Versus operating frequency ( $T_{cr} = 270$  K,  $T_h = 300$  K, and  $P = 17.5$  bar ).

heat exchanger temperature  $T_h = 300$  K and chiller temperature  $T_{cr} = 270$  K). This result confirms that the major pressure drop existed in the regenerator that was almost equal to the total pressure drop.

The effect of shuttle heat loss on the temperature of the working fluid is illustrated in Fig. 9. From Fig. 9, it could be seen that shuttle heat loss has a major effect on the temperature of the gas. The shuttle heat loss has the effect of decreasing hot gas temperature and increasing cold side gas temperature. At a charging pressure of 17.5 bar, hot heat exchanger temperature of 300 K, chiller temperature of 270 K, and an operating frequency of 7.5 Hz, the average hot gas temperature decreased by 14 K, and the average cold gas temperature increased by 10 K when incorporating the shuttle effect in the differential equation. Furthermore, the effects of shuttle heat loss on the overall performance of the refrigerating machine have been evaluated. The cooling power and COP of the refrigerating machine were found respectively as 450.9 W and 77% when shuttle loss was evaluated separately and subtracted from cooling power. On the other hand, the cooling power and COP were found as 342 W and 62% when shuttle heat loss was incorporated in the differential equation.

Fig. 10 demonstrates the effect of charging pressure on performance of cooling machine (cooling power, input power requirement, and COP). As shown in the figure, the input power requirement, cooling power, and COP of the refrigerating machine increased with charging pressure. The slope of COP and cooling power were greater than the slope of the input power requirement. Hence, as charging pressure increased the overall performance of the refrigerating machine increased. This is mainly due to the effect of increasing in mass of working fluid is greater in heat removal rate than the increase of fluid friction with an increase in charging pressure.

Fig. 11 illustrates the variation of required input power, cold power, and COP of the refrigerating machine versus cold temperature. As cold end temperature increased, cooling production and COP increased but the input power requirement decreased. The increasing of cooling power and the decreasing of input power requirement with increasing of cold temperature has a double effect on the COP of a refrigerating machine. As demonstrated in Fig. 11, the slope of COP is relatively higher with respect to cold temperature.

Fig. 12 is a plot of refrigeration performances (input power required, cooling power and COP) versus frequency of the refrigerating machine. From Fig. 12, it is shown that the cooling production and the input power required increased, whereas the COP decreased with operating frequency within the range of analysis. This indicates that the rate of fluid friction power losses are higher than the rate of increase in cooling power due to the increasing of thermodynamic cycle per unit time. The optimum COP will be found at much lower frequency.

## 5. Conclusion

In the present study, a non-ideal second-order numerical model called the modified simple model considering the effects of various losses has been developed for the moderate temperature Stirling refrigerator. The numerical model was later evaluated against the experimental work. The cold production from the numerical analysis and experimental work are found as 427 W and 450 W respectively at a chiller temperature of  $4^\circ\text{C}$  with a relative error of -5%. The COP from numerical analysis and experimental work are found as 0.91 and 0.9 respectively with a relative error of +1%. These results show that the

numerical model is in close agreement with the results of the experiment.

The effect of incorporating shuttle heat loss in the direct differential equation is analyzed as it affects the working condition particularly the temperature of the working gas. The shuttle heat increases the temperature of working gas in the chiller and hence more power is needed to cool down the fluid to the required temperature. This reduces the performance of the refrigerator. Therefore, treating shuttle heat loss independently as any other heat loss will result in an exaggerated wrong performance of cooling. Furthermore, a parametric study to investigate the effects of charging pressure, operating frequency, and cold end temperature on performance was evaluated.

## 6. Acknowledgments

This work has been supported by EIPHI Graduate School (contract ANR- 17- EURE- 0002) and the Region Bourgogne-Franche-Comte, by Bahir Dar Institute of Technology, by the Embassy of France to Ethiopia and the African Union, and by the Ministry of Science and Higher Education of Ethiopia.

## References

- [1] Jacob Wl Kohler. The stirling refrigeration cycle in cryogenic technology. *The Advancement of Science*, 25:261, 1968.
- [2] Alexander Carnegie Kirk. On the mechanical production of cold.(includes plates and appendix). In *Minutes of the Proceedings of the Institution of Civil Engineers*, volume 37, pages 244–282. Thomas Telford-ICE Virtual Library, 1874.
- [3] JWL Köhler and CO Jonkers. Fundamentals of the gas refrigeration machine. *Philips Tech. Rev*, 16(3):69–78, 1954.
- [4] Muluken Z Getie, Francois Lanzetta, Sylvie Bgot, Bimrew T Admassu, and Abdulkadir A Hassen. Reversed regenerative stirling cycle machine for refrigeration application: a review. *International Journal of Refrigeration*, 118:173–187, 2020.
- [5] Jose Egas and Don M Clucas. Stirling engine configuration selection. *Energies*, 11(3):584, 2018.
- [6] Toshio Otaka, Masahiro Ota, Kazuhiko Murakami, and Moriyoishi Sakamoto. Study of performance characteristics of a small stirling refrigerator. *Heat TransferAsian Research*, 31(5):344–361, 2002.
- [7] Ö Ercan Ataer and H Karabulut. Thermodynamic analysis of the v-type stirling-cycle refrigerator. *International Journal of Refrigeration*, 28(2):183–189, 2005.
- [8] Jincan Chen and Zijun Yan. The general performance characteristics of a stirling refrigerator with regenerative losses. *Journal of Physics D: Applied Physics*, 29(4):987, 1996.
- [9] Jincan Chen. Minimum power input of irreversible stirling refrigerator for given cooling rate. *Energy conversion and management*, 39(12):1255–1263, 1998.
- [10] A Razani, C Dodson, and T Roberts. A model for exergy analysis and thermodynamic bounds of stirling refrigerators. *Cryogenics*, 50(4):231–238, 2010.
- [11] Yusuf Tekin and Omer Ercan Ataer. Performance of v-type stirling-cycle refrigerator for different working fluids. *international journal of refrigeration*, 33(1):12–18, 2010.
- [12] JS Lewis, I Chaer, and SA Tassou. Reviews of alternative refrigeration technologies. *Centre for Energy and Built Environment Research, Brunel University (July 2007)*, 2007.
- [13] Sun Lean, Zhao Yuanyang, Li Liansheng, and Shu Pengcheng. Performance of a prototype stirling domestic refrigerator. *Applied Thermal Engineering*, 29(2-3):210–215, 2009.
- [14] Ruijie Li and Lavinia Grosu. Parameter effect analysis for a stirling cryocooler. *International Journal of Refrigeration*, 80:92–105, 2017.
- [15] Alireza Batooei and Ali Keshavarz. A gamma type stirling refrigerator optimization: An experimental and analytical investigation. *International Journal of Refrigeration*, 2018.
- [16] Mohammad Hadi Katooli, Reza Askari Moghadam, and Ahmad Hajinezhad. Simulation and experimental evaluation of stirling refrigerator for converting electrical/mechanical energy to cold energy. *Energy conversion and management*, 184:83–90, 2019.
- [17] Houda Hachem, Ramla Gheith, Fethi Aloui, and Sassi Ben Nasrallah. Optimization of an air-filled beta type stirling refrigerator. *International Journal of Refrigeration*, 76:296–312, 2017.
- [18] Israel Urieli and David M Berchowitz. *Stirling cycle engine analysis*. A. Hilger Bristol, 1984.
- [19] Mojtaba Babaelahi and Hoseyn Sayyaadi. Simple-ii: a new numerical thermal model for predicting thermal performance of stirling engines. *Energy*, 69:873–890, 2014.
- [20] Fawad Ahmed, Huang Hulin, and Aqib Mashood Khan. Numerical modeling and optimization of beta-type stirling engine. *Applied Thermal Engineering*, 149:385–400, 2019.
- [21] Houda Hachem, Ramla Gheith, Fethi Aloui, and Sassi Ben Nasrallah. Technological challenges and optimization efforts of the stirling machine: A review. *Energy Conversion and Management*, 171:1365–1387, 2018.
- [22] Iskander Tlili, Youssef Timoumi, and Sassi Ben Nasrallah. Analysis and design consideration of mean temperature differential stirling engine for solar application. *Renewable Energy*, 33(8):1911–1921, 2008.
- [23] Mohammad H Ahmadi, Mohammad-Ali Ahmadi, and Fathollah Pourfayaz. Thermal models for analysis of performance of stirling engine: A review. *Renewable and Sustainable Energy Reviews*, 68:168–184, 2017.
- [24] Youssef Timoumi, Iskander Tlili, and Sassi Ben Nasrallah. Design and performance optimization of gpu-3 stirling engines. *Energy*, 33(7):1100–1114, 2008.
- [25] M Mahmoodi, J Pirkandi, and A Alipour. Numerical simulation of beta type stirling engine considering heat and power losses. *Iranian Journal of Mechanical Engineering Vol*, 15(2):6, 2014.
- [26] David Gedeon and JG Wood. Oscillating-flow regenerator test rig: hardware and theory with derived correlations for screens and felts. 1996.
- [27] Guozhong Ding, Wenming Chen, Tianyi Zheng, Yongzhen Li, and Yakun Ji. Volume ratio optimization of stirling engine by using an enhanced model. *Applied Thermal Engineering*, 140:615–621, 2018.
- [28] M Costea, S Petrescu, and C Harman. The effect of irreversibilities on solar stirling engine cycle performance. *Energy conversion and management*, 40(15-16):1723–1731, 1999.
- [29] Zhang Cun-Quan, Wu Yi-Nong, Ji Guo-Lin, Liu Dong-Yu, and Xu Lie. Dynamic simulation of one-stage oxford split-stirling cryocooler and comparison with experiment. *Cryogenics*, 42(9):577–585, 2002.
- [30] Steve Djetel-Gothe, Sylvie Bégot, François Lanzetta, and Eric Gavignet. Design, manufacturing and testing of a beta stirling machine for refrigeration applications. *International Journal of Refrigeration*, 115:96–106, 2020.